Journal of Low Temperature Physics, Vol. 138, Nos. 5/6, March 2005 (© 2005)
DOI: 10.1007/s10909-004-2895-y

Ellipsometry of Liquid Helium Films on Gold, Cesium, and Graphite

T. McMillan, J. E. Rutledge, and P. Taborek

Department of Physics and Astronomy, University of California, Irvine, USA
E-mail: Ptaborek@uci.edu

(Received July 22, 2004; revised October 18, 2004)

We have developed a modulated null ellipsometer with sub-monolayer resolution to measure adsorbed liquid helium thin films at temperatures below 4 K. Adsorption isotherms of ^4He on gold, cesium, and graphite are presented. For Au and Cs substrates, the reflecting surface for our ellipsometric measurements is the metallic electrode of a quartz crystal microbalance (QCM). Performing both types of measurements simultaneously on the same substrate provides a direct method of converting the ellipsometric signal into an absolute film thickness without constructing a detailed model of the refractive index of the substrate. Isotherms on gold above and below T_λ, show that the ellipsometric signal is unaffected by the superfluid transition; the ellipsometer measures the total film thickness independent of the superfluid fraction. Isotherms on cesium above the wetting temperature show a prewetting step. Isotherms on clean graphite show steps due to layering.

KEY WORDS: adsorption; ellipsometry; graphite; cesium; QCM; microbalance.

1. INTRODUCTION

Ellipsometry is a widely used, high precision technique for making non-invasive, *in-situ* measurements on thin films and characterizing the optical properties of surfaces. The technique exploits the difference in the complex amplitude reflection coefficients r_p and r_s for light polarized parallel to the plane of incidence (p-polarized) and perpendicular to the plane of incidence (s-polarized). This difference in reflection coefficients implies that, in general, light that is linearly polarized or circularly polarized will become elliptically polarized upon reflection from a conductive surface. The orientation and aspect ratio of the ellipse is a sensitive function of the optical constants $n + ik$ of the substrate and the optical constants

0022-2291/05/0300-0995/0

and thickness of any adsorbed film. If the optical properties and geometry of the reflecting surface are known, the Fresnel equations can be solved for the reflection coefficients r_p and r_s. The elliptical polarization of the reflected beam can be characterized by the ratio of the two reflection coefficients, which is a single complex number. This complex number can be described using two real parameters which are traditionally chosen to be Δ and Ψ defined by

$$\mathrm{Tan}(\Psi)e^{i\Delta} = \frac{r_p}{r_s}. \tag{1}$$

A measurement of Δ and Ψ on a bare substrate provides a direct determination of the optical constants of the substrate. Incident light that is linearly polarized 45° to the angle of incidence, such that the *p* and *s* components of the electric field are equal and in phase, makes a reflected ellipse with orientation Ψ and eccentricity Δ. As a thin film grows on the surface, the measured values of Δ and Ψ change. The resulting change in Δ, $\delta\Delta$, is typically much larger than the corresponding $\delta\Psi$ for thin adsorbed films and is the only measurement required to determine the film thickness provided that the optical index of the film is known. Since only one ellipsometric parameter needs to be determined, a relatively simple form of ellipsometry known as null ellipsometry can be employed.[1] The principle of the technique is to prepare an input beam with elliptic polarization with the appropriate properties so that the reflected beam on the bare substrate is linearly polarized. A linear polarizer in the detection optics is adjusted to obtain a minimum in the signal. As a film grows on the substrate, the reflected beam becomes slightly elliptically polarized and there is a corresponding increase in the intensity of the signal from the crossed polarizer. The signal can be brought back to a null by adjusting a linear polarizer in the input beam optics.

The orientation of the two polarizers determines the parameters Δ and Ψ by the relations,

$$\Delta = 2\mathrm{P}_1 + 90^\circ, \tag{2}$$

$$\Psi = \mathrm{P}_2 \tag{3}$$

in which P_1 refers to the orientation of the input polarizer and P_2 to the output or analyzer polarizer. This is valid when the compensator waveplate has $\lambda/4$ retardation and its pass axis oriented at 45° to the plane of incidence. The angular change required to re-null the signal is $\delta\Delta/2$. The high sensitivity of the technique is related to the ability to adjust the linear polarization with a precision of 0.0001 degree using a Faraday modulator.

In principle, the measured values of $\delta\Delta$ in degrees can be related to a film thickness in Angstroms using a model based on the Fresnel equations. Detailed calculations for a thickening film of helium on an ideal gold substrate show several general features of the dependence of $\delta\Delta$ on film thickness d which are illustrated in Fig. 1. $\delta\Delta$ is a periodic function of film thickness with a characteristic period of order of the wavelength of light. In the thin film regime (which for helium is approximately $d < 350\,\text{Å} \approx 100$ layers), $\delta\Delta$ is approximately linearly proportional to film thickness. It is this proportionality constant which depends on the exact value of n and k for the substrate and film. In our experiments, the reflecting substrate is a gold electrode of a quartz crystal microbalance (QCM). When the adsorbed film is in the normal state and is viscously clamped to the substrate, the QCM provides an alternate measure of the film thickness which can be used to establish the proportionality constant between d and $\delta\Delta$.

Performing high-resolution ellipsometry on helium films inside a cryostat is experimentally challenging. In our apparatus, the optical beam passes through eight windows, each of which can change the transmitted polarization and overwhelm our signal. Helium films are very sensitive to thermal gradients, so our beam is restricted to power levels below $1\,\mu$W. Compared to all other condensed matter, the optical index of liquid helium is very low, with $n \approx 1.028$ for 633 nm light. Since the ellipsometric signal is proportional to $n - 1$, this means that the ellipsometer signal for a given thickness is more than 10 times smaller for helium than for a

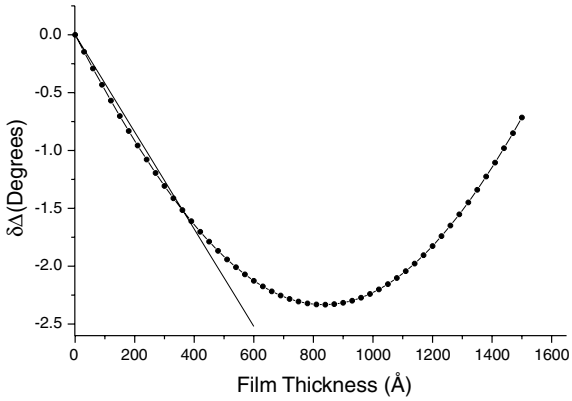

Fig. 1. $\delta\Delta$ as a function of adsorbed film thickness d for helium on gold. The dotted curve is a calculation based on the Fresnel equations using the parameters 632.8 nm light, 50° incidence angle, $n_{\text{Au}} = 0.124 + 3.26i$, $n_{\text{He}} = 1.028$, a fixed second polarizer and the major axis of the $\lambda/4$ plate fixed at 45° to the plane of incidence. $\delta\Delta$ is a periodic function of d. For films less than 350 Å, a linear approximation shown by the straight line is quite accurate.

conventional material such as Kr, which has $n = 1.3$. Calculated values of $\delta\Delta$ for the two materials are compared in Fig. 2.

Despite these difficulties, ellipsometric experiments have been successfully performed with liquid helium.[2,3] All of these previous measurements were performed at saturation and involved films hundreds of layers thick. The focus of these studies was the measurement of the helium film profile as a function of height above the bath,[4–7] measuring the condensation and evaporation rate[8] and detecting third sound.[9] More recently, several groups have constructed cryogenic ellipsometers which work in the liquid nitrogen temperature range to study wetting properties of Xe, Kr, Ar and N_2 on substrates such as silicon and graphite.[10–16] These experiments had sub-monolayer resolution and were able to resolve individual layer-by-layer growth. Recently, experiments by Wu and Hess have demonstrated this same resolution on HD films[17] down to 8.5 K. One of the goals of our experiments was to extend the sub-monolayer resolution achieved for the classical gasses to helium films at temperatures below 4 K. As noted above, the small value of $n - 1$ for helium requires an order of magnitude higher resolution in $\delta\Delta$. Because the ellipsometric signals from helium films are small, it is particularly important to control stray polarization shifts from birefringence in the windows at a level which would not be required for more optically dense materials. Another important concern is the long term stability of the ellipsometric signal. A high resolution isotherm requires measurements at more than 100 pressure values, and since the thermal time constant of our apparatus is several minutes, a typical

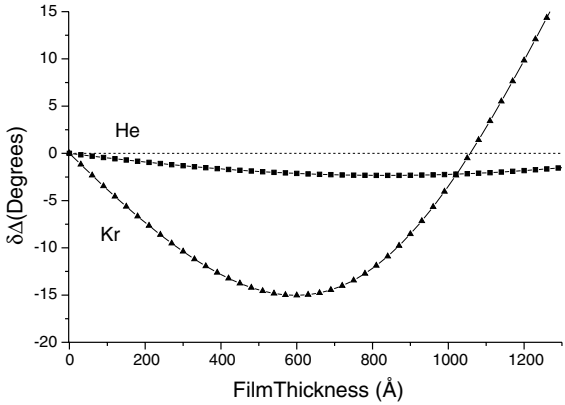

Fig. 2. $\delta\Delta$ as a function of film thickness for He and Kr on gold calculated using $n_{Kr} = 1.3$, and $n_{He} = 1.028$. The slope in the thin film regime is approximately 10 times larger for Kr than for He.

isotherm takes over 12 hours to complete. The techniques we developed for minimizing the effects of birefringence and reducing the drift to less than 0.1 effective layers of helium over a 12 hour period are reported in Ref.18.

One of the motivations for developing ellipsometry with sub-monolayer resolution for helium films is to study the interaction of superfluidity with wetting and prewetting transitions. Perhaps the most commonly used tool for studying superfluid onset in thin helium films is the high Q mechanical oscillator. Both kilohertz frequency torsional oscillators and megahertz quartz oscillators are in widespread use. When the film is in the normal state, these devices measure the total coverage, but in the superfluid state, they measure only the normal component of the film plus some fraction of the superfluid that depends on the tortuosity of the substrate. There are no readily available techniques for making unambiguous measurements of the total coverage once the film has become superfluid. For conventional substrates which are completely wet by helium, this is not a serious drawback since "missing mass" in an oscillator measurement can safely be attributed to decoupled superfluid. For weak and intermediate strength substrates such as cesium and rubidium,[19] however, "missing mass" can be an indication of superfluidity, incomplete wetting, or a combination of the two. Because there are no discontinuities in the optical index at the superfluid transition, ellipsometry has the potential to provide a reasonably direct measure of film thickness in both the normal and superfluid state. By combining QCM and ellipsometer measurements we hope to be able to independently measure the normal fraction and total coverage and thus determine the superfluid fraction. This would allow us to disentangle the effects of wetting and superfluidity in the combined transitions observed in Rb and explore the non-Kosterlitz-Thouless(KT) behavior observed in that system.

Since ellipsometry of thin helium films is not a well established technique, it is important to verify its performance using some standard well characterized systems. Here we report results on ^{4}He films adsorbed on gold and evaporated cesium surfaces measured simultaneously with the ellipsometer and the QCM, and ellipsometer measurements on clean highly ordered pyrolytic graphite (HOPG). Low temperature isotherms on gold show that the ellipsometer signal is not affected by superfluid onset, which is clearly visible in the QCM signal. Isotherms on Cs show a prewetting step in both types of measurements. Ellipsometric isotherms on graphite show steps which reflect layer-by-layer growth. These results verify that the ellipsometer measures the total coverage and is capable of detecting subtle surface phase transitions with sub-monolayer resolution. Preliminary results with an earlier version of the instrument have been reported previously.[20] In Sec. 2 of this paper we provide a complete

description of the current ellipsometer apparatus. In Sec. 3, isotherms obtained with the ellipsometer and the QCM on Au, Cs and graphite, are discussed.

2. APPARATUS

The ellipsometer consists of three parts: the input side to prepare the incident polarization, the output side to analyze the reflected light and an electronic feedback loop to maintain and record the signal. Our particular system is a modulated null ellipsometer, similar to that used by Volkmann and Knorr.[10] The principle is to input just the right elliptically polarized light onto the surface such that the reflected light is linearly polarized. This linearly polarized light is then nulled by the second analyzer polarizer and the intensity is measured with a photomultiplier tube (PMT). In order to use narrow band lockin techniques to improve the signal to noise ratio, the input beam is modulated about the null using a Faraday modulator in the input beam optics. The Faraday modulator rotates the polarization angle by an amount proportional to the current flowing through a solenoid. The PMT response at the modulation frequency is used as an error signal in a feedback loop which controls the DC part of the signal to the Faraday modulator. The DC part of the current in the Faraday modulator solenoid is proportional to $\delta\Delta$ and is the primary experimental quantity of interest.

The layout of the ellipsometer is shown in Fig. 3. The light source for the input beam is 632.8 nm 5 mW HeNe laser with a linearly polarized

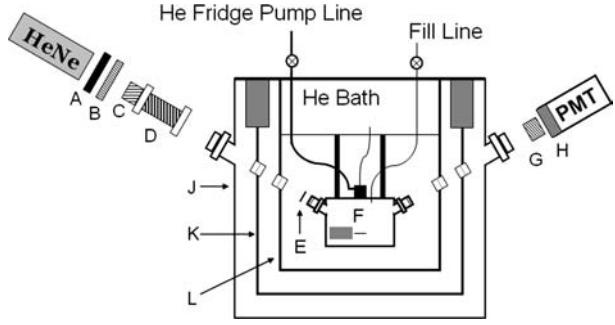

Fig. 3. Experimental apparatus. The OD3 filter(A), $\lambda/4$ plate(B), linear polarizer(C), faraday modulator(D) and $\lambda/4$ plate(E) prepare the input beam. A stepper motor holds and aligns the QCM(F) which the beam reflects off. The second polarizer(G), narrowband filter(H) and PMT analyze and measure the beam. The cryostat consists of a stainless steel vacuum jacket(J), liquid nitrogen radiation shield(K), liquid helium radiation shield(L) and the copper experimental cell in the center.

output. It is convenient to be able to rotate the polarization without rotating the laser, so a simple broadband mica $\lambda/4$ plate, Fig. 3B, with its axis fixed at 45° to the polarization axis of the laser beam is used to transform the beam to circularly polarized. The next component is a Glan–Thompson linear polarizer prism, Fig. 3C, mounted in a standard manual rotation stage. This serves as a coarse adjustment to the input polarization. A circularly polarized input beam allows this polarizer to select out the polarization required with negligible change in intensity. Glan–Thompson polarizers were chosen for their high extinction ratios of 10^{-5}. The high resolution control of the input polarization is provided by the Faraday modulator.

The Faraday modulator, Fig. 3D, consists of a piece of transparent material with a high Verdet constant in a magnetic field. Light transmitted coaxially with the field through the medium will have its polarization rotated by an amount proportional to the length of the medium, Verdet constant and strength of field. Our modulator uses a cylinder of super-precision annealed SF-57 glass,[21] 10 mm diameter by 60 mm length, with a Verdet constant of 21.8 rad m^{-1} $Tesla^{-1}$. The glass is placed inside a solenoid allowing very fine rotations to the polarization to be accomplished by simply changing the current in the coil. In its present configuration the rotation is 2.1 degree/Amp, but this gain can be adjusted by changing the length of the glass or the number of loops in the coil. The coil carries a DC offset which tracks the growth of the film as well as the AC modulation.

The linearly polarized beam which emerges from the Faraday modulator must be converted to elliptical polarization before reflecting off the surface. This is done with a first order quartz $\lambda/4$ plate designed for 632.8 nm light, Fig. 3E. This $\lambda/4$ plate determines the orientation of the input ellipse, while the polarizer determines the eccentricity. Calculations and experiment show that maximum sensitivity and the lowest intensity nulls occur when this $\lambda/4$ plate is oriented so that its optical axis is 45° to the plane of incidence. Although first order quartz wave plates are designed to be insensitive to temperature variations, we found that fluctuations of even a few tenths of a degree in the room temperature produced polarization shifts comparable to those produced by a monolayer of helium. To avoid this problem, the $\lambda/4$ plate is located in the low temperature part of the apparatus on the outside of the experimental cell just above the input window.

The elliptically polarized beam exiting the $\lambda/4$ plate enters the experimental cell and reflects off the electrode of the QCM, Fig. 3F. The reflection shifts the polarization back to linear and then the beam exits the cryostat through another set of windows. The beam then passes through a second

Glan–Thompson linear polarizer, Fig. 3G. As the beam travels through the sequence of nearly parallel windows in the cryostat, multiple reflections are produced so there are several secondary spots exiting the cryostat. A small 1 mm aperture on this second polarizer ensures that only the primary, direct beam is the one that is nulled and passed on to the PMT. If properly nulled this reduces the input beam intensity by a factor of 10^{-5}. Even at a null, however, there is still a measurable picowatt signal.

As the experiment cools, thermal contractions alter the alignment of the QCM with respect to the laser and other optics. To facilitate realignment of the beam and to provide the ability to evaporate films onto both sides of the substrate, the QCM is attached to the cell via a low temperature stepper motor[22] which rotates the QCM about an axis parallel to the plane of incidence. When the experiment has cooled to 4.2 K, the beam is again aligned. The two linear polarizers are then adjusted until the exiting beam has been effectively nulled on a bare surface in vacuum, with no DC current in the Faraday modulator. An absorptive Optical Density(OD) three filter, Fig. 3A, is then placed directly in front of the laser, which reduces the total intensity by a factor of 10^3. This prevents heating of the sample and maintains the signal below the maximum threshold of the PMT. Isotherms have also been performed with an OD two filter using an order of magnitude higher optical power, with no appreciable change in the ellipsometer signal. This shows that no local heating was occurring on the QCM.

The PMT is a Hamamatsu R2949. A narrowband interference filter,[23] Fig. 1G, centered at 632.8 nm is fixed in front of the PMT aperture in order to eliminate the unpolarized white light emitted by the laser. The experiments are typically carried out in a darkened room. The PMT outputs a raw current signal which is converted to a voltage using a Stanford Instruments SR-570 low noise current pre-amplifier. The output voltage signal is then fed into a lock-in amplifier.

The feedback loop that maintains the null is shown in Fig. 4. The reference channel output of the lock-in amplifier provides a modulation at 330 Hz which is chosen to be below the roll-off frequency of the modulator coil. The amplitude of the modulation oscillates the polarization by $\pm 0.15^\circ$. An important advantage of making the measurement in this AC fashion is that the error signal is insensitive to fluctuations in the laser intensity; the error depends only on the position of the null, but not on the value of the signal at the null. The error is processed by a PID controller which produces a DC signal required to restore the null. This DC correction is added to the AC modulation using an analog adder circuit. The output of the adder is converted to a current using a Kepco bipolar operational power supply and sent back to the modulator. The ellipsometer

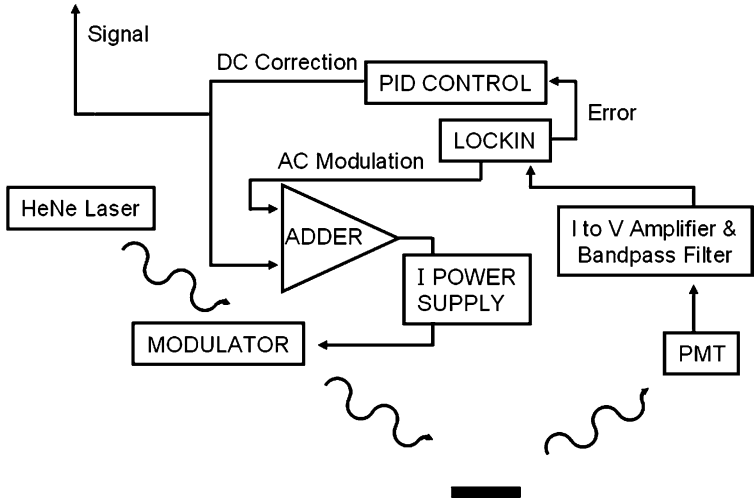

Fig. 4. Schematic of feedback loop and electronics. AC modulation gets added to the DC correction and sent to the Faraday modulator.

is continuously kept nulled by this feedback loop. The feedback loop has a time constant of a few seconds, which is short compared to the time between points in an isotherm. The actual recorded signal comes from a voltmeter that measures the DC correction just before being added to the AC modulation.

The QCM sits in a copper experimental cell in the center of an optical cryostat. The cell is thermally isolated and hangs from thin walled stainless steel legs. A refrigerator attached to the top of the cell has a high impedance capillary running back up to the helium bath on one side and a larger bellows pumping line on the other. By varying the pumping speed and the input power to a small heater on the top of the cell, temperatures between 1.3 and 5 K can be reached and maintained to within 0.001 K. Two radiation shields are needed for this cryostat; an inner one in thermal contact with the liquid helium bath, Fig. 3L, and an outer shield, Fig. 3K, in contact with the liquid nitrogen jacket. This reduces the heat load on the cell and helps with temperature stability but adds four additional windows through which the beam must be transmitted. Residual birefringence and stress in these windows must be reduced to avoid unintended retardation of the polarization.[18]

3. RESULTS AND DISCUSSION

We have used the QCM and the ellipsometer to measure ^{4}He isotherms for three representative types of substrates: gold, which is a strong

binding substrate with continuous and complete wetting; cesium, which is a weak substrate with a wetting and prewetting transition; and HOPG, which has uniform crystallites which leads to layer-by-layer growth of many materials[13,15–17] including helium.[36] Figure 5 shows a comparison of the QCM and ellipsometer signals on gold at T = 2.34K. The pressure is given in units of P/P_0, or percentage of saturation. Neither the QCM nor the ellipsometer measures coverage directly. In the case of the QCM, the coverage is determined from the primary measured quantity Δf_{meas}, which is the change in resonant frequency from its value at $P = 0$. The frequency shift Δf_{meas} is due to the additional hydrodynamic mass of the adsorbed

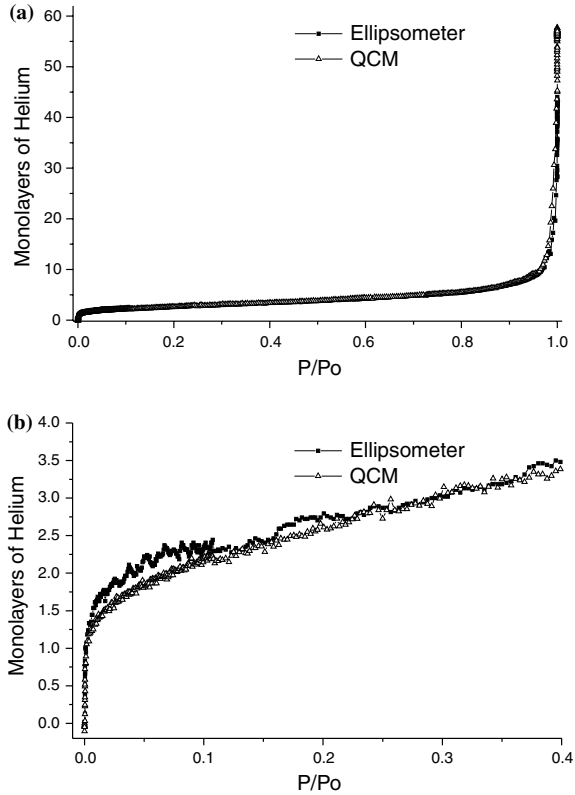

Fig. 5. Comparison of helium film thickness on gold as a function of reduced pressure measured with the QCM and the ellipsometer at T = 2.34 K. P_0 is the saturation pressure. The QCM and ellipsometer thickness are derived from measured quantities as described in the text. (a) shows the two measurements agree very well over the entire pressure range from vacuum to saturation. (b) shows a closer view of the first few layers.

liquid film and the vapor surrounding the QCM. The vapor contributes a term to the mass loading and therefore the frequency shift which is proportional to $\sqrt{P}$. There is also a small correction to the properties of the quartz crystal itself which is proportional to P. The measured frequency shift can be expressed[24] as:

$$\Delta f_{\text{meas}} = \Delta f_{\text{film}} + \frac{2 f_o \sqrt{\eta_{\text{vapor}}\, \rho_{\text{vapor}}}}{N \pi \mathrm{R_Q}} + \alpha f_o P, \tag{4}$$

where the second term is the hydrodynamic mass of the vapor and the third term is the pressure correction. The acoustic impendence of quartz, $\mathrm{R_Q}$, is $8.9 \times 10^6\,\mathrm{kg\,m^{-2}s^{-1}}$. Our SC cut QCMs have a fundamental, $N=1$, resonant frequency, f_o, in vacuum of 5.5 MHz. Helium isotherms measured with SC cut QCMs are qualitatively similar to those measured with AT cut QCMs.[35] Substituting the density, ρ_{vapor}, and viscosity η_{vapor}, for helium at 2.3 K, the hydrodynamic vapor contribution is $0.21\sqrt{P}$ (Hz) with P in units of Torr. We have measured the pressure dependence of the resonant frequency of our SC cut crystals to be $\alpha = \delta f / f_0 \delta P$ to be 1.33×10^{-9} $\mathrm{Torr^{-1}}$ at 2.3 K, making the last term $0.0073P$ (Hz) with P in Torr units. These are relatively small corrections that result in a total reduction of the bulk film thickness at saturation of about 3%.

Once the correct Δf_{film} is calculated it can be converted to a film thickness, d. We found it more useful to record this value in terms of layers of helium than Angstroms. The frequency shift as a function of d can be calculated using:

$$\Delta f_{\text{film}} = \frac{-4 f_o^2 \rho_{\text{He}} d}{N \mathrm{R_Q}}. \tag{5}$$

If we assume d for one layer of liquid helium is 3.57 Å then Eq. (3) gives a Δf_{film} of 0.66 Hz/Layer at 2.3 K.

The primary measured quantity in the ellipsometer is $\delta\Delta$, which can be related to the effective film thickness using a model based on the Fresnel equations. The computed film thickness, shown in Fig. 1, depends on the optical constants for the gold substrate, for which we used the bulk values[25] $n = 0.124$ and $k = 3.26$ for 633 nm light at room temperature. In principle, the ellipsometer signal also depends on the optical constants of the vapor, but calculations show that variations in the computed film thickness due to this effect are negligible in the range of vapor pressures for our experiments. For the thin helium films of interest here, the linearized model which leads to a relation of the form $d_{\text{Ellip}} = A\delta\Delta$ is sufficiently accurate. When computed in this way, d_{QCM} is approximately 4% larger than d_{Ellip}. We believe this discrepancy is due to slight differences between

the optical constants of our evaporated thin film gold substrate measured at low temperature and the literature values for bulk gold at room temperature. k, which measures the dissipative part of the optical response, is particularly sensitive to surface roughness and temperature dependent loss mechanisms. The thickness values d_{QCM} and d_{Ellip} can be brought into agreement by assuming the real part of the optical index n has the same value for our gold film substrate as for bulk gold, but that the imaginary part $k = 3.86$ is approximately 20% larger. The ellipsometric thickness shown in Figs. 5 and 6 was computed using these values.

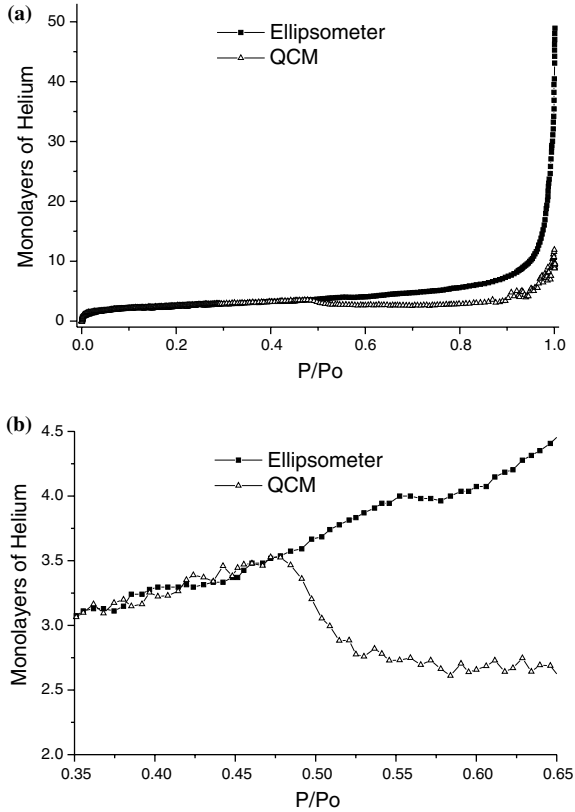

Fig. 6. Comparison of the QCM and ellipsometer thickness for helium adsorption on bare gold at T = 1.52K. (a) shows the full isotherm and (b) shows a closer view of the KT transition showing superfluid onset. As the film becomes superfluid, the QCM signal drops because it measures only ρ_n while the ellipsometer smoothly increases because it measures the total coverage.

Figure 5a shows that the ellipsometric and QCM thickness are virtually indistinguishable from each other. The most prominent feature in Fig. 5a is the rapid increase in film thickness near saturation at $P/P_0 = 1$, which is the hallmark of a wetting film. A more subtle feature is the small step near $P/P_0 = 0$, which is the buildup of approximately two strongly bound solid-like layers at low chemical potential. This feature is shown in more detail in Fig. 5b, which shows that the ellipsometer and QCM thickness differ by at most a few tenths of a layer.

Figure 6 shows a similar comparison of the QCM and ellipsometric coverage as a function of pressure at T = 1.52K, sufficiently below the 2.17 K λ point. At low pressures, the two curves are almost coincident until $P/P_0 \approx 0.5$, when a drop in the QCM signal signifies superfluid onset via a KT transition. The QCM can only measure the fraction of the film that is viscously coupled to it, namely the normal fraction, ρ_n. The ellipsometer measures the total coverage and does not distinguish between the superfluid fraction, ρ_s, and ρ_n. A closer view of the transition in Fig. 6b shows that the ellipsometric thickness is smooth and continuous through the transition, and that the thickness resolution of the QCM and the ellipsometer are both approximately 0.1 layers. The difference between these two curves represents ρ_s, the superfluid fraction.

We have also used our ellipsometric technique to study isotherms of helium on cesium. Cesium is a weak binding substrate[26] and is the only material for which a wetting transition with ^{4}He has been observed. The wetting temperature is approximately 2 K.[27,28,31] Below this temperature, the surface coverage remains below a few layers even at saturation. Isotherms slightly above this wetting temperature display a first order prewetting transition in which the coverage abruptly jumps from a value of a few layers to tens of layers at a pressure distinctly less than P_0; this transition represents a coexistence region of a thick and thin phase on the substrate which is analogous to the liquid–vapor transition in 3D. As the pressure is further increased, the film thickness diverges in a manner similar to the strong binding substrate case. Because of this unusual behavior, the helium–cesium system has been investigated using a variety of techniques.[29–33]

Our cesium films were prepared by *in-situ* evaporation. A glass ampule containing the cesium is broken at 4.3 K inside the experimental cell. A resistive heater is used to heat the ampoule which is attached to the cell through a Macor holder for weak thermal conduction. The cesium is evaporated onto both sides of the QCM. The thickness of the deposited cesium is monitored using the QCM, and is approximately 300 layers per side. Throughout the evaporation the temperature of the cell walls is kept below 10 K which ensures UHV conditions and prevents contamination of the film.

Figure 7 shows a comparison of the ellipsometer and QCM signal for an isotherm on evaporated Cs at T = 1.52K. The interpretation of the QCM signal is independent of substrate, but the ellipsometer signal depends on the optical properties of the substrate which are different for Cs and Au. The room temperature index of refraction for a cesium film at 633 nm is $0.26 + 1.24i$.[34] We find that an accurate agreement between the ellipsometer and the QCM signals can be obtained by adjusting the imaginary part of the Cs index slightly to $0.26 + 1.31i$; this value was used to convert the measured values of $\delta\Delta$ into the ellipsometric thickness shown in Fig. 7. Figure 7a shows the thickness for the entire range of reduced pressure. A

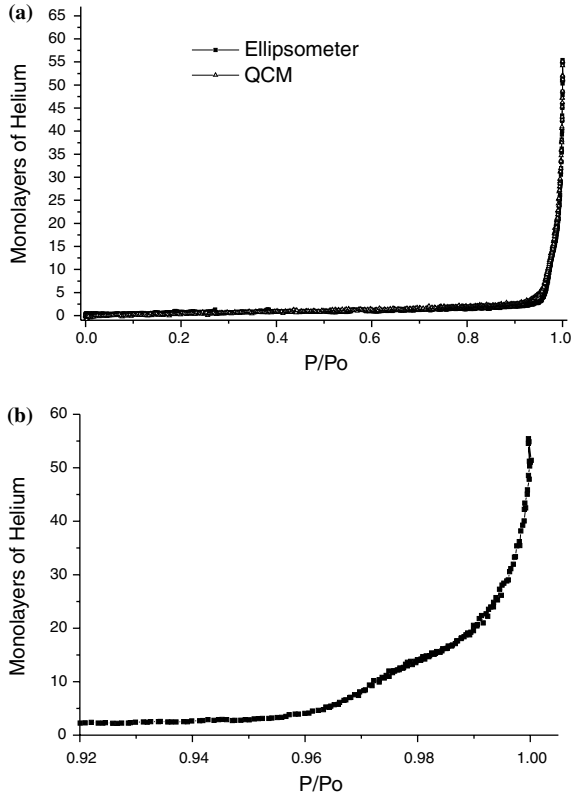

Fig. 7. Helium adsorption isotherm on an evaporated cesium film at 2.34 K. (a) shows that the QCM and ellipsometer signals are essentially indistinguishable over the entire pressure range. No solid-like layers form at low pressures, and the film remains thin until the prewetting step at $P/P_0 = 0.96$. (b) shows a detailed view of the ellipsometer signal in the prewetting region.

characteristic feature of isotherms on Cs at all temperatures is the absence of the two layer step which can be seen in the low pressure regime of Fig. 6a. On Cs the film thickness increases gradually with pressure until $P/P_0 = 0.96$ where the prewetting step occurs. At this temperature the helium film is in the normal state, consequently the ellipsometer and QCM thickness are virtually indistinguishable throughout the entire pressure range. The ellipsometer is capable of detecting this rather subtle surface phase transition. Both the small size of the prewetting step and its extreme sensitivity to temperature gradients make it an experimentally difficult phenomenon to observe. Resolving this step confirms that local heating by the laser beam is not a significant thermodynamic perturbation. Figure 7b shows the ellipsometer signal in the prewetting region in more detail.

We have also used the ellipsometer to study the growth of helium films on HOPG. The graphite surface was cleaned at 4 K in vacuum by using a laser pulse from a frequency doubled Q switched YAG laser with a wavelength of 532 nm, a total energy of approximately 5 mJ and a pulse width of 7 nsec. The beam was focused to a spot size of approximately 1 mm^2 and rastered across the graphite surface. A similar technique was used in Ref. 11. The ellipsometric isotherm is shown in Fig. 8. Note that the the first two layers fill at essentially zero pressure, and that the ellipsometrically determined thickness is approximately 2.6 layers, which indicates a 30% increase in the local density near the surface. Subsequent

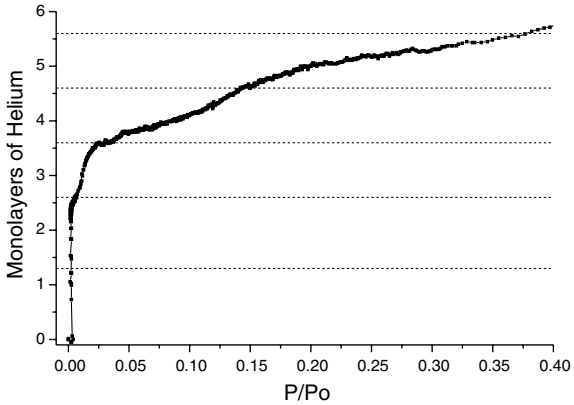

Fig. 8. Helium adsorption isotherm on laser cleaned HOPG at T = 1.34K. The units on the vertical axis are statistical monolayers at bulk liquid density; the dashed horizontal lines are estimates of layer completion points. The near vertical rise at zero pressure is the completion of the first two layers. The third layer is complete at a reduced pressure of approximately 0.02, and the 4th layer is complete at a reduced pressure of approximately 0.15.

layers have normal density. The results are qualitatively similar to volumetric isotherms on graphite foam.[36]

4. SUMMARY AND CONCLUSIONS

The experiments reported here represent the first ellipsometrically determined helium isotherms. For helium films in the normal state, we find that the ellipsometric thickness and the thickness determined by a QCM are always proportional. The proportionality factor depends on the real and complex parts of the optical index of the substrate. Using room temperature literature values for the optical properties typically leads to a discrepancy in the ellipsometric film thickness of order 4%. We believe this is due to sensitive dependence on temperature variation and surface morphology, particularly for the imaginary part of the index. Our current ellipsometer is optimized to measure a single ellipsometric parameter, $\delta\Delta$. We plan to make changes to our apparatus to allow us to measure both Δ and Ψ, and thus to determine the optical constants of the bare substrate *in-situ* at low temperature. For the experiments reported here, however, we experimentally established the proportionality factor between the two signals by performing our ellipsometric measurement directly on the surface of a QCM. A single readjustment of the value of the imaginary part of the index yielded very good agreement between the ellipsometer thickness and the QCM thickness over the entire range of reduced pressure. The precision of both measurements is approximately 0.1 layer. Comparison of the QCM and ellipsometer signal for superfluid films confirms that the ellipsometer measures the total film thickness independent of the superfluid fraction. We have also used the ellipsometer to detect the prewetting step on Cs.

Ellipsometry has several experimental advantages over conventional methods of detecting helium film thickness. It has sub-monolayer resolution over a wide range of absolute film thickness and is independent of superfluidity. It can be used on almost any flat reflective substrate, including bulk metals and single crystal surfaces. We are confident that these experimental advantages will find application in future studies with helium films.

ACKNOWLEDGMENTS

This work was supported by NASA NAG 81437 and NSF DMR 997159.

REFERENCES

1. R. M. A. Azzam and N. M. Bashara, *Ellipsometry and Polarized Light*, Elsevier Science (1999).
2. D. V. Osborne, *J. Phys. Condens. Matter* **1**, 289 (1988).
3. C. C. Matheson, J. G. Wright, R. Gundermann, and H. Norris, *Surf. Sci.* **56**, 196 (1976).
4. E. J. Burge and L. C. Jackson, Proc. R. *Soc. Lon. Ser. A* **205**, 270 (1951).
5. A. C. Ham and L. C. Jackson, *Proc. R. Soc. Lon. Ser. A* **240**, 243 (1957).
6. O. T. Anderson, D. H. Liebenberg, and J. R. Dillinger, *Phys. Rev.* **117**, 39 (1960).
7. D. Hemming, *Can. J. Phys.* **49**, 2621 (1971).
8. D. G. Blair and C. C. Matheson, *Physica. B* **180**, 541 (1975).
9. C. W. F. Everitt, K. R. Atkins and A. Denenstein, *Phys. Rev. Lett.* **8**, 161 (1962).
10. U. G. Volkmann and K. Knorr, *Surf. Sci.* **221**, 379 (1989).
11. J. W. O. Faul, U. G. Volkmann, and K. Knorr, *Surf. Sci.* **227**, 390 (1990).
12. U. G. Volkmann and K. Knorr, *Phys. Rev. Lett.* **66**, 473 (1991).
13. H. S. Youn, X. F. Meng, and G. B. Hess, *Phys. Rev. B* **48**, 14556 (1993).
14. S. Igarashi, Y. Abe, T. Hirayama, and I. Arakawa, *SPIE* **2873**, 203 (1996).
15. G. Quentel, J. M. Rickard, and R. Kern, *Surf. Sci.* **50**, 343 (1975).
16. G. Quentel and R. Kern, *Surf. Sci.* **55**, 545 (1976).
17. H. Wu and G. B. Hess, *Phys. Rev. B* **57**, 6720 (1998).
18. T. McMillan, P. Taborek, and J. E. Rutledge, *Rev. Sci. Instr.* **75**, (2004).
19. J. A. Phillips, D. Ross, P. Taborek, and J. E. Rutledge, *Phys. Rev. B* **58**, 3361 (1998).
20. T. McMillan, P. Taborek, and J. E. Rutledge, *J. Low Temp. Phys.* **134**, 303 (2004).
21. Schott Optical Glass, Inc, 400 York Ave.,Duryea, PA 18642
22. Phytron VSS.91.200.6-UHVC
23. OptoSigma narrowband interference filter Part #079–1380
24. M. J. Lea and P. Fozooni, *J. Low Temp. Phys.* **56**, 25 (1984).
25. M. J. Weber, *Handbook of Optical Materials* CRC Press (2003).
26. E. Cheng, M. W. Cole, J. Dupont-Roc, W. F. Saam, and J. Treiner, *Rev. Mod. Phys.* **65**, 557 (1993).
27. J. E. Rutledge and P. Taborek, *Phys. Rev. Lett.* **69**, 937 (1992).
28. P. Taborek and J. E. Rutledge, *Phys. Rev. Lett.* **71**, 263 (1993).
29. R. B. Hallock, *J. Low Temp. Phys.* **101**, 31 (1995).
30. P. Stefani, J. Klier, and A. F. G. Wyatt, *Phys. Rev. Lett.* **73**, 692 (1994).
31. J. Klier, P. Stefani, and A. F. G. Wyatt, *Phys. Rev. Lett.* **75**, 3709 (1995).
32. V. Iov, J. Klier, and P. Leiderer, *Physica B* **329**, 242 (2003).
33. A. Prevost, E. Rolley, and C. Guthmann, *Phys. Rev. Lett.* **83**, 348 (1999).
34. N. V. Smith, *Phys. Rev. B* **2**, 2840 (1970).
35. R. Brada, H. Chayet, and W. I. Glaberson, *Phys. Rev. B* **48**, 12874 (1993).
36. G. Zimmerli, G. Mistura, and M. H. W. Chan, *Phys. Rev. Lett* **68**, 60 (1992).